

## Interaction between oppositely charged micelles or globular proteins

J. Z. Wu, D. Bratko, H. W. Blanch, and J. M. Prausnitz

*Department of Chemical Engineering, University of California, Berkeley, California 94720  
and Chemical Sciences Division, Lawrence Berkeley National Laboratory, Berkeley, California 94720*

(Received 19 April 2000)

Monte Carlo simulations and the hypernetted chain theory are used to study the interaction between spherical macroions of opposite charge immersed in a solution of monovalent or divalent simple electrolyte. These calculations represent the first step toward studying phase behavior and precipitation kinetics in solutions containing a mixture of macroions with positive and negative net charges. The potential of mean force between colloidal particles is determined as a function of colloid-colloid separation. In addition to having an opposite sign, the calculated potential of mean force is found to be stronger and longer-ranged than observed in the case of equally charged macroparticles. The difference is more pronounced in the presence of divalent counterions and is especially noticeable when we compare distinct Coulombic and hard-core collision contributions to the interaction between equally and oppositely charged colloids. The present observations suggest the dominance of attractive forces between globally neutral but electrostatically heterogeneous macroparticles. While our numerical results cannot be successfully analyzed by existing theories, they provide useful guidance and benchmark data for the development of advanced analytic descriptions.

PACS number(s): 61.25.Hq, 61.20.Ja, 61.20.Qg

### I. INTRODUCTION

The phase behavior and kinetic properties of ionic colloids are determined by the interplay of short-ranged van der Waals attraction and long-ranged electrostatic forces between macroions [1–4]. Understanding these interactions has been the objective of numerous theoretical studies [5–37]. In view of the instability of mixtures containing macroions with opposite charges, the vast majority of theoretical descriptions has been concerned with solutions of macroions with equal charges, or polydisperse mixtures of colloids carrying charges of equal sign. The screened Coulombic repulsion among the particles has repeatedly been identified as a vital factor responsible for the apparent stability of ionic colloidal dispersions. Traditional theories such as the Derjaguin, Landau, Verveij, and Overbeek (DLVO) theory [5], and its derivatives like the Sogami-Ise theory [6], rely on a set of simplifications, including the neglect of ion-ion correlations and the linearization of Boltzmann weights for calculating ionic distributions. A known result of these simplifications is the approximate potential of mean force between colloidal particles,  $W(r)$ , which typically takes the form of the direct Coulombic interaction for the two bare polyions multiplied by a screening function that depends solely on the distance and the ionic strength of the solution. The reversal of the charge on either of the two macroions is reflected in the reversal of the sign of the potential of the mean force (determined by the product of the two charges,  $Z_1$  and  $Z_2$ ), but the form of  $W(r)$  is not changed in any other way. Nonlinear analytical methods like those based on integral equation theory [7,10,12–14,16–18,20,21,24,28], along with simulation studies [11,15,19,21,22,29–37] of equally charged colloids, point to a more complex behavior. In view of the importance of the potential of mean force toward understanding colloid solubility and aggregation kinetics, it is of interest to extend these calculations to mixtures containing oppositely

charged macroparticles. Here we describe a simulation study of the interaction between a pair of macroions with opposite charges immersed in a solution of symmetric monovalent or divalent simple electrolyte. Using the simulation technique developed in earlier work [33,35], we determine the distance dependence of the potential of mean force between macroions with opposite charges as well as distinct physical contributions to the overall interaction. Our results show that the overall potential of mean force is only approximately opposite to that observed in the case of equal macroion charges. The magnitudes of the pair potential and the forms of radial decay for the two scenarios are, however, noticeably different. The difference is especially pronounced in the presence of a divalent electrolyte. Individual contributions to the overall interaction reveal considerable deviations from simple sign reversal even in monovalent salt solutions. The observed differences are interpreted in terms of markedly different distributions of simple ions in the region around and between the polyions, and related effects on electrostatic screening and on the imbalance in the pressure the counterions exert on macroion surfaces. Our calculations provide different insights into the mechanism of macroion-macroion interaction that should help in interpretations of phase behavior and association dynamics in processes involving macroions with opposite charges, such as, for example, selective precipitation from protein mixtures and titration of a mixture of proteins with different isoelectric points. In addition, the numerical results we present offer benchmark data for alternative analytic theories. The remainder of the article is organized as follows. In Sec. II, we describe the model and the simulation technique we use to calculate separate contributions and the total colloid-colloid interaction. Section III surveys and discusses simulation results. In concluding Sec. IV, we summarize our findings and indicate a few practical implications of interest for future work.

## II. MODEL AND METHOD

A dilute colloidal solution is represented using the primitive model of an asymmetric electrolyte [38] containing four different species, macroions of diameter  $\sigma_M$  and charge  $Z_M$  or  $-Z_M$ , and symmetric salt comprising cations and anions of diameter  $\sigma_C$  and charges  $Z_C$  and  $-Z_C$ , respectively, where  $Z_C=1$  or  $2$ . Solvent molecules are not explicitly considered; the presence of the solvent is apparent only through the permittivity  $\varepsilon$  of the system. The macroions and small ions interact among themselves by Coulombic forces and hard-core repulsion. The pair potential  $u_{ij}$ , for species  $i$  and  $j$ , is

$$u_{ij}(r_{ij}) = \infty, \quad \text{if } r_{ij} < \sigma_{ij}, \quad \sigma_{ij} = \frac{(\sigma_i + \sigma_j)}{2}$$

and

$$u_{ij}(r_{ij}) = \frac{Z_i Z_j e^2}{4\pi\varepsilon\varepsilon_0 r_{ij}} \quad \text{otherwise,} \quad (1)$$

where  $r_{ij}$  represents the center-to-center distance between particles,  $Z_i e$  is the charge on ion  $i$ ,  $\varepsilon_0$  is the permittivity of vacuum, and  $\varepsilon$  is the dielectric constant of the solvent. Since we consider pair interaction between macroions at high dilution, our simulation cell contains only two macroions and a large number of simple ions. In all calculations, the size of the box exceeds the length of  $5-10 \kappa^{-1}$ , where  $\kappa^{-1}$  is the Debye-Huckel screening length. Sampling over a single pair of macroions, the intercolloidal potential of mean force cannot be calculated accurately from the macroion-macroion radial distribution. In addition, we are interested in separate calculations of Coulombic and collision contributions to the mean interaction between the particles. For both reasons, the force is sampled directly according to the procedure introduced in our earlier work [33,35]. The method is based on the relation

$$F(r) = -\frac{du_{MM}(r)}{dr} - \left\langle \sum \frac{du_{iM}(r_{iM})}{dr_{iM}} \right\rangle + F_{\text{hs}}, \quad (2)$$

where the angular brackets denote the ensemble average,  $r$  is the separation between the two macroions, and  $r_{iM}$  is the distance between a small ion  $i$  and a macroion  $M$ . The first term on the right-hand side (rhs) of Eq. (2) is the direct Coulombic force between the two macroions, the second term comprises Coulombic forces between the macroions and small ions, and the third term represents the mean force due to the collisions between the macroions and surrounding simple ions. The collision force can be calculated from the imbalance of the pressure exerted on a colloidal particle according to the expression [32,39]

$$F_{\text{hs}} = -k_B T \int_S \sum \rho(S) \vec{n}(S) d\vec{S}. \quad (3)$$

Equation (3) requires knowledge of the macroion-small ion contact density  $\rho(S)$  as a function of the position on the macroion surface,  $S$ ;  $\vec{n}(S)$  is the outward normal unit vector on the surface, and the sum is over all ionic species present in the solution. This method requires the calculation of the

angle dependent macroion-small ion distribution functions and subsequent extrapolation to contact distance. In preceding articles [33,35], we have proposed an alternative technique that circumvents this lengthy procedure by calculating the average collision force from collision probabilities due to test displacements of the macroion. According to the analysis presented in Ref. [35], the collision force can be expressed as

$$F_{\text{hs}} = -k_B T \lim_{\delta r \rightarrow 0^+} \frac{\langle N_c \rangle}{\delta r} - k_B T \lim_{\delta r \rightarrow 0^-} \frac{\langle N_c \rangle}{\delta r}, \quad (4)$$

where  $N_c$  denotes the average number of macroion-small ion collisions due to small trial displacements  $\delta r$  or  $-\delta r$ . Extrapolation to vanishingly small  $\delta r$  is not necessary if sufficiently small values of  $\delta r$  are used in the simulation. The range of appropriate values of  $\delta r$  has to be determined empirically. For most of the conditions considered in the present study, the magnitude  $\delta r \sim 1\%$  of  $\sigma_M$  turned out to be sufficiently small to eliminate any significant finite size effect while keeping collisional probability sufficiently high to secure satisfactory statistical accuracy.

The sampling of the force between macroions was carried out using canonical ensemble Monte Carlo simulations for a set of fixed macroion-macroion distances. Following earlier work [33,35], the macroions were fixed at prescribed positions along the cell diagonal and the boundary effects were taken into account using Ewald periodic conditions [40,41]. We sampled over the configurations of simple ions following the standard Metropolis procedure [40]. Having determined the average force between macroions as a function of separation, the potential of mean force  $W(r)$  was calculated by straightforward integration of the force from separations with vanishingly weak interaction to a set of selected distances  $r$  [42]. The length of the production runs was adjusted according to the desired statistical accuracy of calculated forces estimated from the reproducibility of our results. In general, the calculated collision force was found to converge several times more slowly than the electrostatic term. The statistical error in calculated forces at small macroion-macroion separations was typically below 1–2%. In systems containing several hundred simple ions, each of the production runs required about  $10^8$  attempted configurations.

## III. RESULTS AND DISCUSSION

In what follows, we present the force, energy, and potential of mean force profiles obtained by Monte Carlo simulations for five model systems. Each of these systems comprises a pair of macroions of diameter  $\sigma_M = 2$  nm and absolute charge  $|Z_M| = 20$ , neutralizing counterions of diameter  $\sigma_c = 0.2$  nm and charge  $Z_C = 1$  or  $2$ , and specified concentration  $c_s$  of a symmetric monovalent or divalent simple salt. The size and the valency of salt ions equal those of the counterions. In addition to simulation results, we include the predictions of the hypernetted chain integral equation [43] (HNC) for macroion-macroion potentials of mean force at similar conditions, but at a lower net charge than that of the macroions,  $\forall Z_M = 10$ , at which the theory still produces reliable results. In all systems, the temperature and permittivity correspond to aqueous solutions at ambient conditions. Characteristic model parameters are collected in Table I. System

TABLE I. Characteristic model parameters of simulated systems.  $Z_a$  and  $Z_b$  are the charges of the two macroions, and  $Z_c$  and  $Z_d$  the charges of simple ions.  $\sigma_M$  and  $\sigma_C$  denote the diameter of the macroions and small ions, and  $c_{\text{salt}}$  is the concentration of the simple electrolyte. Temperature  $T=298$  K and relative permittivity  $\epsilon_r=78.5$  are assumed in all systems. MC stands for Monte Carlo simulation.

System	Method	$Z_a$	$Z_b$	$\sigma_M$ (nm)	$Z_c$	$Z_d$	$\sigma_C$ (nm)	$c_{\text{salt}}$ (mol dm $^{-3}$ )
1	HNC	-10	-10	2	1	-1	0.42	0.1
2	HNC	10	-10	2	1	-1	0.42	0.1
3	HNC	-10	-10	2	2	-2	0.42	0.1
4	HNC	10	-10	2	2	-2	0.42	0.1
5	MC	-20	-20	2	1	-1	0.40	0.1
6	MC	20	-20	2	1	-1	0.40	0.1
7	MC	-20	-20	2	2	-2	0.40	0.1
8	MC	20	-20	2	2	-2	0.40	0.1
9	MC	20	-20	2	2	-2	0.40	0.025

pairs (1,2), (3,4), (5,6), and (7,8) provide a comparison of the potentials of mean force between equally and oppositely charged macroions at otherwise identical conditions. Comparison between systems 6 and 9 illustrates the role of simple ion valency, 1 or 2, at a fixed ionic strength of the solution.

We begin the survey of our results by inspecting the predictions of the HNC integral equation theory for solutions with macroions of equal or opposite charges. The theory provides radial distribution functions among solute species  $i$  and  $j$ ,  $g_{ij}(r) = 1 + h_{ij}(r)$  as solutions of Ornstein-Zernike equations [43]

$$h_{ij}(r_{ij}) = \beta c_{ij}(r_{ij}) + \sum_k \rho_k \int_V c_{ik}(r_{ik}) h_{jk}(r_{jk}) dr_k$$

with

$$c_{ij}(r_{ij}) = -u_{ij}(r_{ij})/k_B T + h_{ij}(r_{ij}) - \ln[1 + h_{ij}(r_{ij})] \quad (5)$$

for all species pairs  $ij$  in the solution. Since we are considering an isolated macroion pair in a salt solution, in the present case, the sum in the convolution term of Eq. (5) contains only two terms with  $k=1$  or 2 corresponding to simple salt cations and anions. The HNC approximation has often been applied to model ionic colloids [7,10,12,13,16–18,20,21]. While it has provided useful insights to both the static and dynamic [18] properties of moderately charged colloids, and has been found to be in quantitative agreement with experiment in studies of weakly ionized globular proteins [21], the HNC theory becomes less reliable with increasing surface charge density of the macroions [16,18]. In the presence of colloidal particles with opposite charges, considered in this work, the applicability of the method is limited to macroion charges  $Z_M$  of the order 10 (at  $\sigma_M \sim 2$  nm).

Figure 1 compares the HNC potentials of mean force between equally and oppositely charged colloids of valency  $Z_M=10$  in the presence of 0.1 mol dm $^{-3}$  monovalent or divalent salt at negligible colloid concentration, systems 1–4 of Table I. Details of the method adhere to our previous work [18] and are not repeated here. The absolute value of the potential of mean force is shown for easier comparison. For both the equally (thick lines) and oppositely (thin lines) charged colloids, the screening of interaction is much more

efficient in divalent (solid lines) than in monovalent salt (dashed lines). Besides the difference in the sign, the interaction is also consistently stronger (in absolute value) and longer-ranged for oppositely charged macroion pairs. The difference is explained in terms of weaker electrostatic screening due to the reduction in counterion concentration in the region between two adjacent macroions of opposite charge brought at a small separation. In view of the reduced accuracy of the HNC theory at increased macroion charge density, in Fig. 1 we present only results pertaining to the low-charge regime where the reliability of the theory has been well established [16,18]. The limitations of the HNC theory at increased macroion charge are illustrated in Figs. 2 and 3 where we compare intercolloidal potentials of mean force from simulations with HNC predictions for conditions identical to those in systems 1–4 of Table I but with doubled macroion charge. Comparison with simulation confirms that the HNC theory is not suitable for quantitative studies at higher macroion charges where the interesting differences between screening mechanisms of interactions among equally and oppositely charged macroions are more pronounced. For this reason, and because HNC calculations cannot provide three-particle distributions, we continue to focus

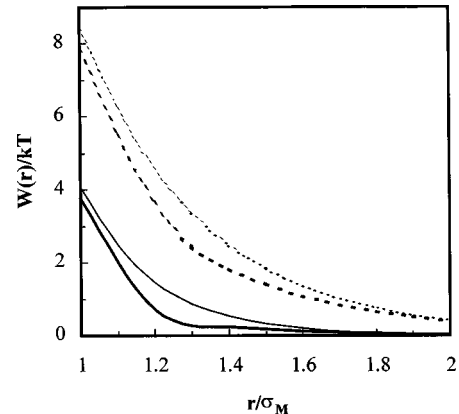


FIG. 1. Hypernetted chain (HNC) predictions for the potentials of mean force between two macroions of equal charges  $Z_M = -10$  (thick lines) or opposite charges (10, -10) (thin lines) in 0.1 mol dm $^{-3}$  solution of symmetric monovalent (dashed lines) or divalent (solid lines) salt. Results for attracting (oppositely charged) macroions are multiplied by  $-1$  for easier comparison.

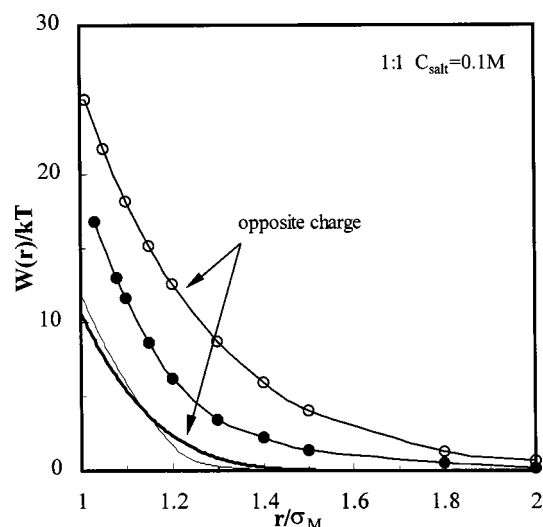


FIG. 2. Potential of mean force between two macroions of equal charges  $Z_M = -20$  (solid symbols) or opposite charges (20,  $-20$ ) (open symbols) in  $0.1 \text{ mol dm}^{-3}$  solution of symmetric monovalent salt (systems 5 and 6 of Table I) from the simulation. Thin and thick curves without symbols represent results from HNC theory for equal and opposite charges, respectively. Results for attracting (oppositely charged) macroions are multiplied by  $-1$  for easier comparison.

on the results of Monte Carlo simulation.

Figure 4 illustrates the distribution of simple ions in the vicinity of a pair of oppositely charged macroions at separation  $r = 1.3\sigma_M$  from simulation. Solution parameters correspond to those of system 8 in Table I. Each of the macroions is surrounded by a cloud of concentrated salt ions of opposite charge, with cations predominantly accumulated around the macroanion and anions around the macrocation. The ion dis-

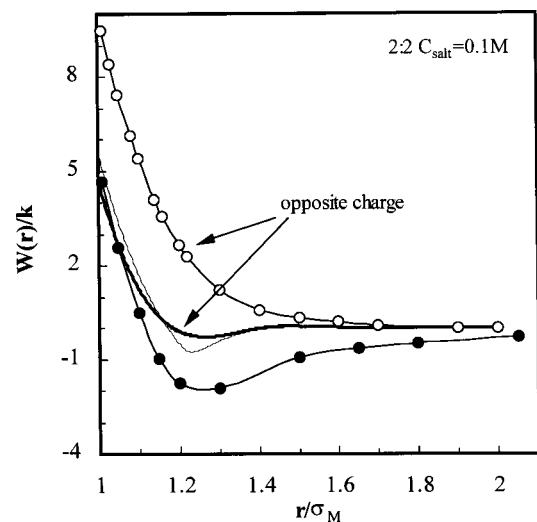


FIG. 3. Potential of mean force between two macroions of equal charges  $Z_M = -20$  (solid symbols) or opposite charges (20,  $-20$ ) (open symbols) in  $0.1 \text{ mol dm}^{-3}$  solution of symmetric divalent salt (systems 7 and 8 of Table I) from the simulation. Thin and thick curves without symbols represent results from HNC theory for equal and opposite charges, respectively. Results for attracting (oppositely charged) macroions are multiplied by  $-1$  for easier comparison.

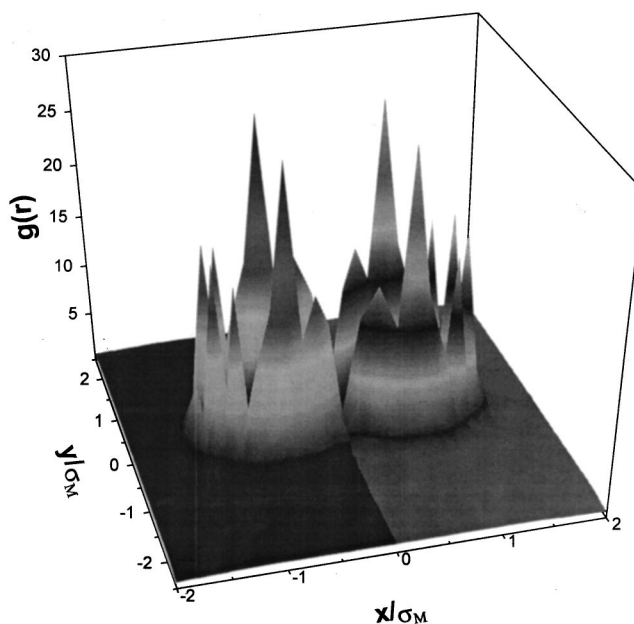


FIG. 4. Distribution of divalent simple ions surrounding a pair of oppositely charged macroions with charges (20,  $-20$ ) at salt concentration  $0.1 \text{ mol dm}^{-3}$  (system 8 of Table I). Center-to-center distance  $r = 1.3\sigma_M$ . Here,  $g(r)$  represents the radial distribution function between the macroions and simple ions from the salt. The  $xy$  plane contains the symmetric axes of the system.

tribution is, however, not isotropic. The angular distribution of small ions around each macroion peaks at the direction perpendicular to the axis connecting the two macroions and also remains relatively high along macroion surfaces pointing away from the neighboring macroion. While the separation between the macroions is sufficient to easily accommodate a layer of small ions between them, the concentration of small ions in the intervening region is negligibly small because the attractive interaction between either of the macroions and a simple ion merely cancels the repulsion with the other macroion. When far apart, the two oppositely charged macroions are effectively screened, each by its own atmosphere of neutralizing small ions. As the two macroions are brought closer, their charge is partly neutralized by the charge of the adjacent macroion and a fraction of counterions is released from the ionic atmosphere of each macroion. Clearly, the large contact distance of the macroions,  $\sigma_M > (\sigma_M + \sigma_C)/2$ , results in higher energies of macroion pairs devoid of counterions in comparison to separated macroions neutralized by a thin shell of counterions. The entropic penalty involved in atmospheric binding of small ions is, however, sufficiently high to render the former scenario more favorable, leading to an attractive macroion-macroion potential. The opposite is true for macroions with charges of equal sign. Here, the energetics favors smaller separations that allow the same counterions to interact favorably with both macroions at the same time. Again, it is the entropy cost associated with the accumulation of small ions in overlapping ionic atmospheres between the macroions that is ultimately responsible for the overall repulsion. Qualitatively, the above mechanism is contained in DLVO theory [5]. Applying the Gibbs-Helmholtz relation to the DLVO potential of mean force between a pair of macroions, the energy can

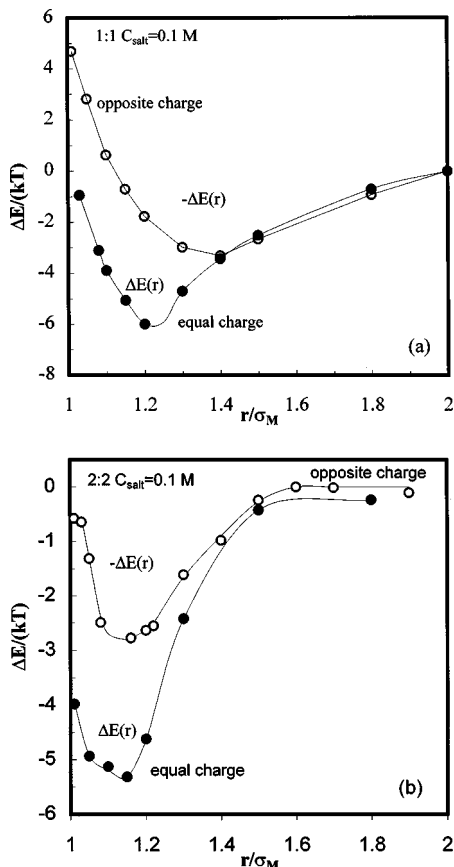


FIG. 5. (a) Energy of interaction for a pair of equally (solid symbols) or oppositely (open symbols) charged macroions of absolute charge  $|Z_M|=20$  in  $0.1 \text{ mol dm}^{-3}$  solution of symmetric monovalent salt (systems 5 and 6) as a function of distance  $r$ . (b) Similar plot for systems 7 and 8 where salt is divalent.

be obtained as a function of macroion-macroion separation. With the possible exception of near contact distances, the sign of this pair energy is opposite to that of the potential of mean force and displays an extremum at a separation of the order of the Debye screening length  $1/\kappa$ . Simulation energy profiles shown in Fig. 5 are consistent with the above picture. They pertain to systems 5–8 of Table I, when the two macroions having equal (systems 5 and 7) or opposite (systems 6 and 8) charges. For repelling macroions (equal charge), the energy of interaction is *attractive* at all separations, with the minimum at the distance corresponding to a monolayer of counterions between the macroions. For attractive, oppositely charged macroions, the energy alone is *repulsive* over most distances, with the extremum observed at a somewhat bigger separation than that found in the equal-charge scenario. The shift in the peak position toward greater distances is explained in terms of a weaker ionic screening characteristic for oppositely charged macroions as indicated in our discussion of the HNC potentials of mean force. The effects of simple ion valency on energy and force profiles are illustrated in Fig. 6, where we collected simulation results for oppositely charged macroions in  $0.1 \text{ mol dm}^{-3}$  monovalent salt, as well as in divalent salt solutions of either the same concentration or equal ionic strength (systems 6, 8, and 9 of Table I). While the energy dependence on the distance remains similar, as seen in Fig. 5, there is a much shorter

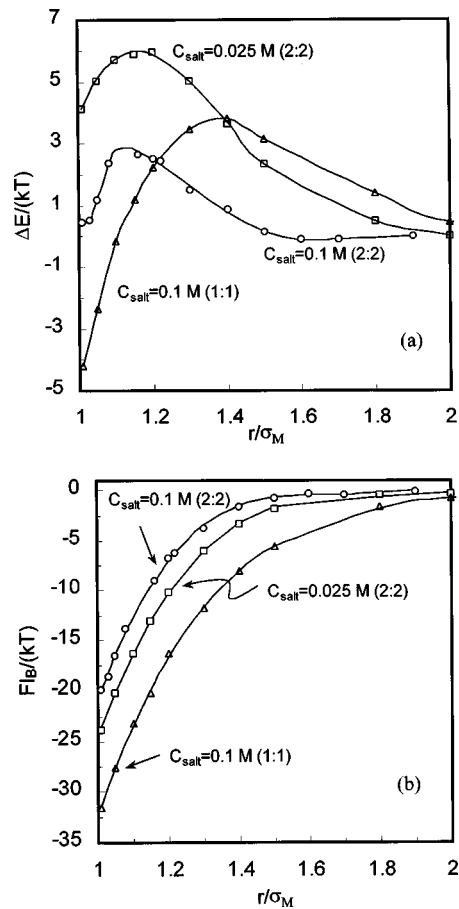


FIG. 6. (a) Energy of interaction for a pair of oppositely charged macroions of absolute charge  $|Z_M|=20$  in  $0.1 \text{ mol dm}^{-3}$  solution of symmetric monovalent salt (system 6, triangles),  $0.1 \text{ mol dm}^{-3}$  solution of divalent salt (system 8, circles),  $0.025 \text{ mol dm}^{-3}$  solution of symmetric divalent salt (system 9, squares) as a function of distance  $r$ . (b) Mean force between macroions for the same systems.  $l_B$  is Bjerrum length ( $0.714 \text{ nm}$  at present conditions).

screening length (deduced from the position of the energy maximum) in the presence of divalent ions than with monovalent salt at the same ionic strength.

In simulation, the potential of mean force can be calculated from the force profile for a macroion pair. Later, we will discuss macroion-macroion potentials obtained in this way. First, we analyze the results for intermacroion forces to extract further insights into the different mechanisms that contribute to the overall interaction. In Figs. 7 and 8, we present the radial dependence of total macroion forces, as well as separate Coulombic and collision contributions. Results in Fig. 7 pertain to solutions with monovalent salt, systems 5 and 6 of Table I, while those in Fig. 8 correspond to divalent salt, systems 7 and 8. In all cases, the forces for the oppositely charged case are multiplied by  $-1$  for easier comparison with the corresponding equal-charge system. The total force is generally of greater magnitude and decays more slowly in the opposite-charge case, in agreement with earlier observations (*vide supra*). Inspection of Coulombic contributions shows that the change in range is primarily due to weaker electrostatic screening. A further qualitative difference in the radial dependence of Coulombic forces is observed by comparing the net forces between equally and op-

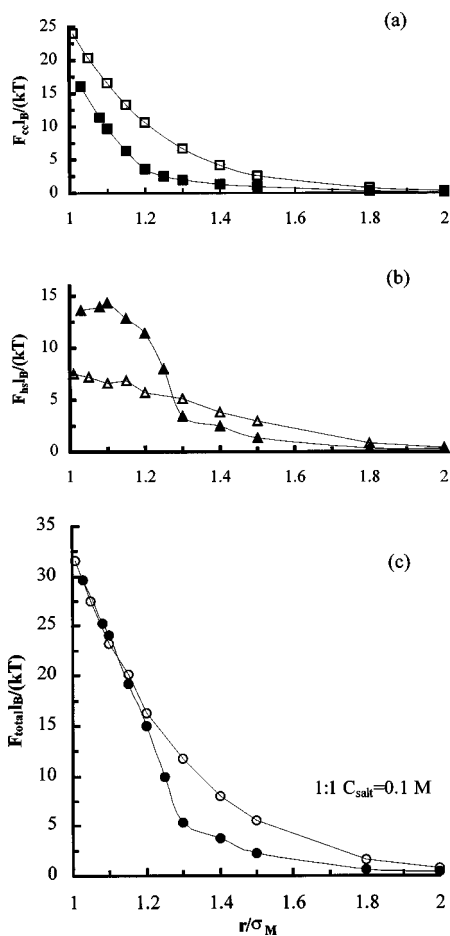


FIG. 7. Mean force between two macroions of equal charges  $Z_M = -20$  (solid symbols) or opposite charges (20,  $-20$ ) (open symbols) in  $0.1 \text{ mol dm}^{-3}$  solution of symmetric monovalent salt (systems 5 and 6 of Table I). Circles, triangles, and squares denote the total force, and the Coulombic and collision contributions, respectively. Results for attracting (oppositely charged) macroions are multiplied by  $-1$  for easier comparison.

positely charged macroions in divalent salt solution. While the predominantly repulsive force acting between equally charged macroions passes through a shallow attractive minimum, the Coulombic force between oppositely charged macroions is monotonically attractive. The reason for the difference lies in the ion correlation mechanism responsible for the attraction in the equal-charge case. These correlations can, at certain conditions, overturn the overall repulsion [12–14]. They remain attractive, albeit weaker, upon reversal of the charge on either of the macroions. The biggest difference between the equal- and opposite macroion charge cases is seen in the collision contribution to the overall force. This term arises from imbalance in the pressure that the simple ions exert on macroion surfaces. With equally charged macroions, the counterions crowd in the region *between* the large ions [33,35], giving a strong repulsive force. When the macroions carry opposite charges, small ions flee the intervening region while they accumulate at *opposite* surfaces. This change in ion distribution leads to an attractive collision term whose magnitude is somewhat smaller than the corresponding repulsive contribution to the force when the two macroions have the same charge. As a result of stronger electrostatic screening in the case of equally charged macroions, the

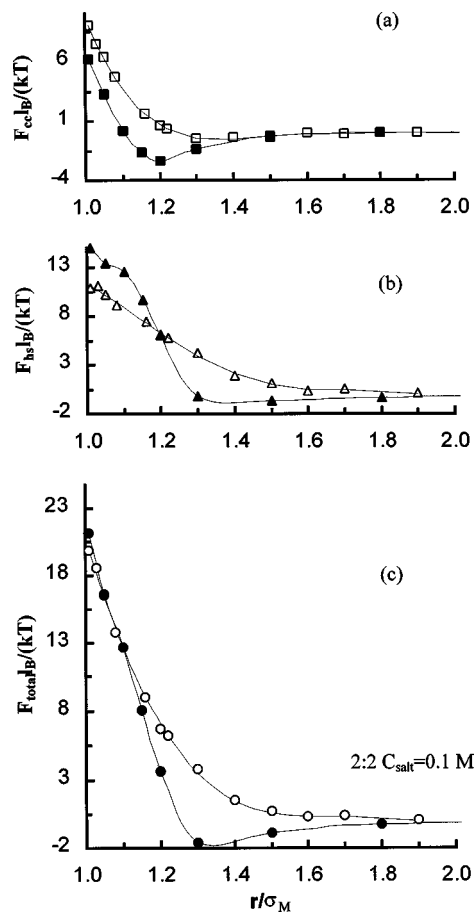


FIG. 8. Mean force between two macroions of equal charges  $Z_M = -20$  (solid symbols) or opposite charges (20,  $-20$ ) (open symbols) in  $0.1 \text{ mol dm}^{-3}$  solution of symmetric divalent salt (systems 7 and 8 of Table I). Circles, squares, and triangles denote the total force, and the Coulombic and collision contributions, respectively. Results for attracting (oppositely charged) macroions are multiplied by  $-1$  for easier comparison.

absolute value of the attractive force between oppositely charged colloids mostly exceeds the repulsion between macroions of equal charge at otherwise identical conditions.

For many purposes, the most useful measure of the overall interaction is the potential of mean force between the macroions. In our simulation, potentials of mean force are determined by integration of the overall force [42] from large distances to a desired separation  $r$ . Potential profiles corresponding to simulation systems 5–8 of Table I are plotted in Figs. 2 and 3. Regardless of the valency of the simple salt, attractive potentials of mean force between oppositely charged macroions are notably stronger (in absolute value) than the repulsive potentials between equally charged macroions of the same absolute charge. This behavior conforms with results from the HNC theory shown in Fig. 1, while it contradicts predictions of classical electrostatic theories, including DLVO and Sogami-Ise models [5,6]. Development of advanced theories that would extend the range of applicability of integral equation descriptions is therefore particularly inviting when considering colloid mixtures containing macroions of opposite charges. An experimental situation of this kind can emerge during titration of a mixture of proteins with different isoelectric points. For planar geometry, this

scenario has been considered by surface force apparatus measurements [44] and by mean-field theory [45]. While there exist reliable experimental data for repulsive interaction among equally charged spherical colloids [46,47], we are not aware of measurements of force profiles for attracting oppositely charged macroions. The differential electrophoresis technique developed most recently [48], however, appears ideally suited to test the predictions of the present study. Another experimentally relevant case concerns attractions between globally neutral but electrostatically heterogeneous surfaces or macroparticles. In view of our present results, attractive electrostatic forces between domains of opposite charge are generally expected to outweigh repulsions between domains carrying charges of equal sign; this expectation can play an important role in processes like aggregation of polyampholytic proteins or polyelectrolyte adsorption.

#### IV. CONCLUDING REMARKS

We report computer simulations of the pair interaction between equally and oppositely charged pairs of spherical macroions in an aqueous solution containing low-molecular weight electrolyte of valency 1 or 2. To the best of our knowledge, similar calculations have not yet been reported. The conditions of observation include the regime where even equally charged macroions can be attractive to each other if the counterion-counterion coupling and concomitant correlation effects are sufficiently strong. In practically relevant situations, such a scenario can be realized in divalent salts. Mean field theories like the DLVO theory, based on the Poisson-Boltzmann equation, cannot capture the ion-ion correlation effects. In the literature, it is often proposed that such theories retain the ability to reproduce essential physics if macroion charge undergoes appropriate renormalization [49]. This implies weaker interactions but the general form of the potential of mean force is presumed to be unaffected by charge renormalization. Similarly, the reversal of the charge on either of the macroions would merely replace repulsion by equally strong attraction while the form of the decay and the range of the interaction would remain unchanged. However, our calculations show that the form and the magnitude of the force profile for a pair of macroions

with opposite charges can be considerably different from those observed in the equal charge case. The differences arise from reduction of the counterion density in the ionic atmosphere of oppositely charged macroions in comparison to the atmosphere surrounding a pair of macroions of equal charge. This reduction results in higher internal energy, but the entropy gain associated with the release of simple ions is sufficient to give rise to the overall attraction. The same mechanism has been revealed by mean-field calculations for electrostatic complexation between ionized proteins and inverted micelles with an oppositely charged shell [50]. For that system, it provided the only successful interpretation of measured [51] maxima in the strength of protein or reversed micelle interaction as a function of protein charge. The exactly opposite mechanism leads to repulsion between equally charged macroions. This picture is consistent with mean-field DLVO theory and is verified by present calculations of the energy as a function of the distance between the macroions carrying equal or opposite charges. The asymmetry in the strength and range of the interaction between colloidal entities with equal charges compared with oppositely charged pairs of the same absolute value suggests the presence of an overall attraction between electrostatically heterogeneous macroparticles or proteins with a nonuniform distribution of ionic groups [52]. If adjacent macroparticles comprise domains that are dominated by local charge density of different signs, the net interaction will be dominated by attractions between oppositely charged domains that are somewhat stronger and of longer range than the repulsions between the domains of equal charge. These observations should be of relevance to interpretations of electrostatic effects on protein-membrane interaction as well as on the thermodynamics and kinetics of colloid or protein precipitation in salt solutions.

#### ACKNOWLEDGMENTS

Financial support for this work was provided by the National Science Foundation and the U.S. Department of Energy (Basic Energy Sciences). We thank Per Linse and Jacob Israelachvili for pointing out references [44,45] and the supercomputing centers, NPACI at San Diego and NERSC at LBNL, for generous allocations of computing time.

- 
- [1] D. F. Evans and H. Wennerstrom, *The Colloidal Domain: Where Physics, Chemistry and Technology Meet* (Wiley, New York, 1999).
- [2] D. H. Everett, *Basic Principles of Colloidal Science* (Royal Society of Chemistry, London, 1988).
- [3] J. Israelachvili, *Intermolecular & Surface Forces* (Academic Press, London, 1992).
- [4] K. Z. Schmitz, *Macroions in Solution and Colloidal Suspension* (VCH Publishers, New York, 1993).
- [5] J. Verwey and J. Th. G. Overbeek, *Theory of the Stability of Lyophobic Colloids* (Elsevier, Amsterdam, 1948).
- [6] I. Sogami and N. Ise, *J. Chem. Phys.* **81**, 6320 (1984).
- [7] G. N. Patey, *J. Chem. Phys.* **72**, 5763 (1980).
- [8] M. Teubner, *J. Chem. Phys.* **75**, 1907 (1981).
- [9] M. J. Grimson and G. Rickayzen, *Chem. Phys. Lett.* **86**, 71 (1982).
- [10] P. Linse and B. Jönsson, *J. Chem. Phys.* **78**, 3167 (1983).
- [11] L. Guldbrand, B. Jönsson, H. Wennerstrom, and P. Linse, *J. Chem. Phys.* **80**, 2221 (1984).
- [12] R. Kjellander, S. Marcelja, *Chem. Phys. Lett.* **112**, 49 (1984).
- [13] R. Kjellander, S. Marcelja, *J. Chem. Phys.* **82**, 2122 (1985).
- [14] G. Senatore and L. Blum, *J. Phys. Chem.* **89**, 2676 (1985).
- [15] D. Bratko, B. Jonsson, and H. Wennerstrom, *Chem. Phys. Lett.* **128**, 449 (1986).
- [16] L. Belloni, *Chem. Phys.* **99**, 43 (1985).
- [17] M. Lozada-Cassou and D. Henderson, in *Micellar Solutions and Microemulsions: Structure, Dynamics and Statistical Thermodynamics*, edited by S. H. Chen and R. Rajagopalan (Springer, New York, 1990), p. 29.
- [18] D. Bratko, H. L. Friedman, and E. C. Zhong, *J. Chem. Phys.*

- 85**, 377 (1986); D. Bratko, H. L. Friedman, S. H. Chen, and L. Blum, *Phys. Rev. A* **34**, 2215 (1986).
- [19] C. E. Woodward, B. Jonsson, and T. Akesson, *J. Chem. Phys.* **84**, 5145 (1988).
- [20] J. Rescic, V. Vlachy, and A. D. J. Haymet, *J. Am. Chem. Soc.* **112**, 3398 (1990).
- [21] D. Bratko, D. Wang, and S. H. Chen, *Chem. Phys. Lett.* **163**, 239 (1990); D. Bratko and D. Henderson, *Electrochim. Acta* **36**, 1761 (1991).
- [22] J. P. Valteau, R. Ivkov, and G. M. Torrie, *J. Chem. Phys.* **95**, 520 (1991).
- [23] R. Kjellander, T. Åkesson, B. Jönsson, and S. Marcelja, *J. Chem. Phys.* **97**, 1424 (1992).
- [24] O. Spalla and L. Belloni, *Phys. Rev. Lett.* **74**, 2515 (1995).
- [25] L. Belloni and O. Spalla, *Ber. Bunsenges. Phys. Chem.* **100**, 905 (1996).
- [26] R. Kjellander, *Ber. Bunsenges. Phys. Chem.* **100**, 894 (1996).
- [27] G. N. Patey, *Ber. Bunsenges. Phys. Chem.* **100**, 885 (1996).
- [28] B. Y. Ha and A. Liu, *Phys. Rev. Lett.* **79**, 1289 (1997).
- [29] N. Grønbech-Jensen, R. J. Mashl, R. F. Bruinsma, and W. M. Gelbart, *Phys. Rev. Lett.* **78**, 2477 (1997).
- [30] B. Hribar and V. Vlachy, *J. Phys. Chem. B* **101**, 3457 (1997); *ibid.* **104**, 4218 (2000).
- [31] V. Lobaskin and P. Linse, *J. Chem. Phys.* **109**, 3530 (1998); J. Rescic and P. Linse, *J. Phys. Chem. B* **104**, 7585 (2000).
- [32] E. Allahyarov, I. D'Amico, and H. L. Löwen, *Phys. Rev. Lett.* **81**, 1334 (1998).
- [33] J. Wu, D. Bratko, and J. M. Prausnitz, *Proc. Natl. Acad. Sci. U.S.A.* **95**, 15 169 (1998).
- [34] N. Grønbech-Jensen, K. M. Beardmore, and P. Pincus, *Physica A* **261**, 74 (1998).
- [35] J. Wu, D. Bratko, H. W. Blanch, and J. M. Prausnitz, *J. Chem. Phys.* **111**, 7084 (1999).
- [36] P. Linse and V. Lobaskin, *Phys. Rev. Lett.* **83**, 4208 (1999).
- [37] B. Hribar and V. Vlachy, *Biophys. J.* **78**, 697 (2000).
- [38] H. L. Friedman, *Ionic Solution Theory* (Wiley, New York, 1962).
- [39] R. Dickman, P. Attard, and V. Simonia, *J. Chem. Phys.* **107**, 205 (1997).
- [40] M. P. Allen and D. J. Tildesley, *Computer Simulation of Liquids* (Clarendon Press, Oxford, 1987).
- [41] D. Frenkel and B. Smit, *Understanding Molecular Simulation* (Academic Press, London, 1996).
- [42] J. S. Bader and D. Chandler, *J. Chem. Phys.* **96**, 6423 (1992).
- [43] H. L. Friedman, *A Course in Statistical Mechanics* (Prentice Hall, Englewood Cliffs, NJ, 1985).
- [44] D. E. Leckband, F. J. Schmitt, J. N. Israelachvili, and W. Knoll, *Biochemistry* **33**, 4611 (1994).
- [45] B. Jonsson and J. Ståhlberg, *Colloids Surf., B* **14**, 67 (1999).
- [46] A. E. Larson and D. G. Grier, *Nature (London)* **385**, 230 (1997).
- [47] D. G. Grier, *Nature (London)* **393**, 621 (1998).
- [48] J. L. Anderson, D. Velegol, and S. Garoff, *Langmuir* **16**, 3372 (2000).
- [49] S. H. Chen and E. Y. Sheu, in *Micellar Solutions and Microemulsions: Structure, Dynamics and Statistical Thermodynamics*, edited by S. H. Chen and R. Rajagopalan (Springer, New York, 1990), p. 3.
- [50] D. Bratko, A. Luzar, and S. H. Chen, *J. Chem. Phys.* **98**, 445 (1988); *Bioelectrochem. Bioenerg.* **20**, 291 (1988).
- [51] K. E. Goklen and T. A. Hatton, *Sep. Sci. Technol.* **22**, 831 (1987).
- [52] O. D. Velev, E. W. Kaler, and A. M. Lenhoff, *Biophys. J.* **75**, 2682 (1998).